Supporting Information

for

Oxidation and Degradation of WS_2 Monolayers Grown by NaCl-Assisted Chemical Vapor Deposition: Mechanism and Prevention

Yao-Pang Chang[1], Wei-Bang Li[2,3], Yueh-Chiang Yang[1], Hsueh-Lung Lu[1], Ming-Fa Lin[3], Po-Wen Chiu[1]*, and Kuang-I Lin[2]*

[1]Department of Electrical Engineering, National Tsing Hua University, Hsinchu 30013, Taiwan

[2]Core Facility Center, National Cheng Kung University, Tainan 70101, Taiwan

[3]Department of Physics, National Cheng Kung University, Tainan 70101, Taiwan

Correspondence and request for materials should be addressed to K.-I.L. (email: kilin@mail.ncku.edu.tw) or to P.-W.C. (email: pwchiu@ee.nthu.edu.tw).

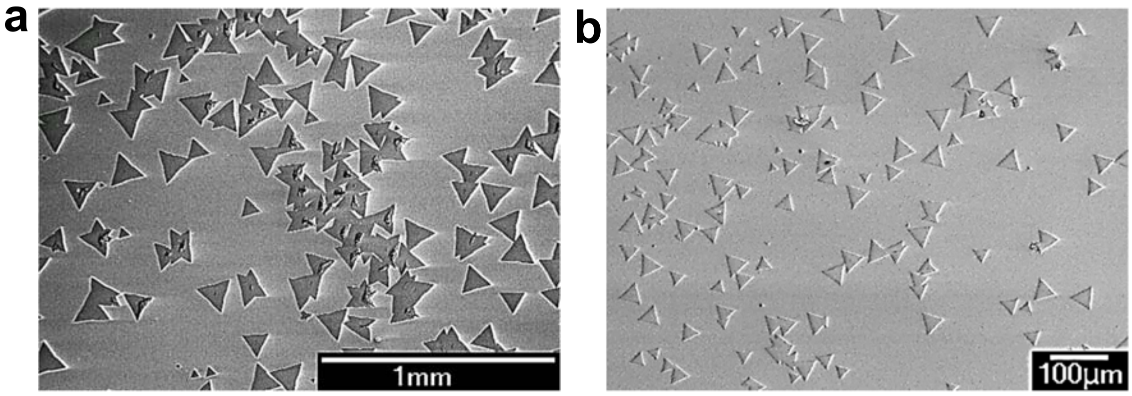

Figure S1. SEM images of WS_2 samples made (a) with NaCl assistant and (b) without NaCl assistant.

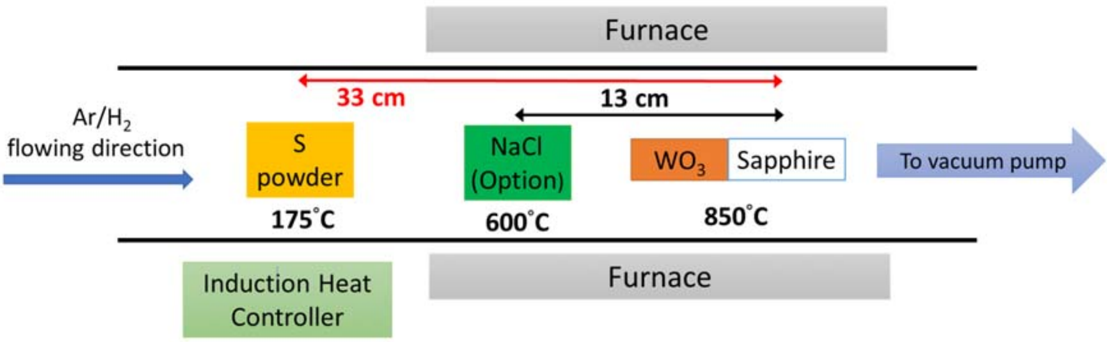

Figure S2. Schematics of the homemade chemical vapour deposition in this work. NaCl is an optional ingredient in this study (please find the details of the experiment).

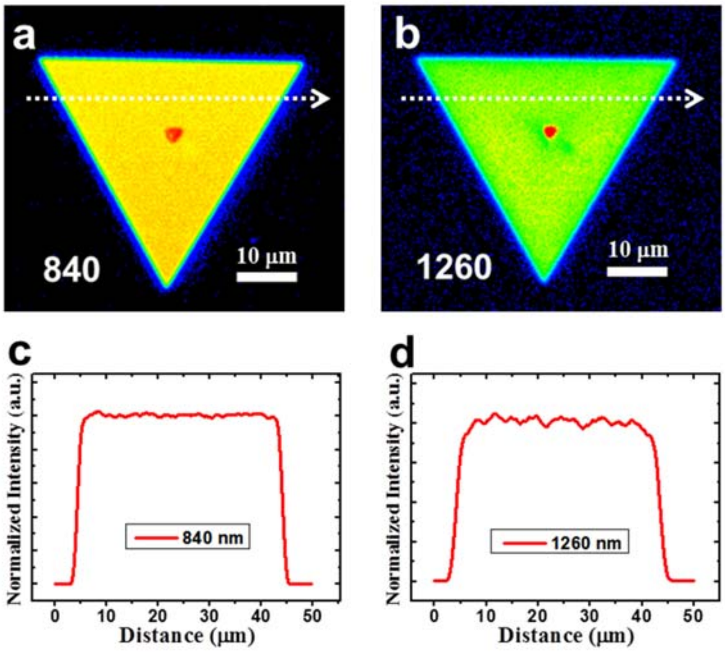

Figure S3. Intensity profile analysis of Figure 1d,f. Both intensity profiles are flat, indicating that there was no photooxidation caused by the SHG laser scanning. In (d), the slight fluctuation is due to the 1260 nm wavelength excitation, and the signal-to-noise ratio is worse than that of 840 nm.

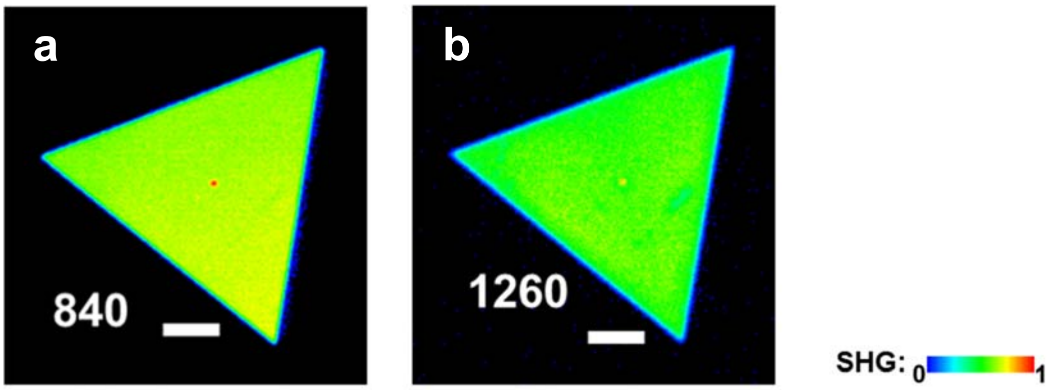

Figure S4. SHG images of a fresh NaCl-assisted WS_2 monolayer before the PL mapping excited at (a) 840 and (a) 1260 nm with fluence of ~3.1×10^6 and 5.1×10^7 Jm^{-2}, respectively. They did not show any dark spots, indicating that there was no photooxidation caused by the SHG laser scanning. SHG intensity is normalized and shown with a rainbow color scale. Scale bar, 10 μm.

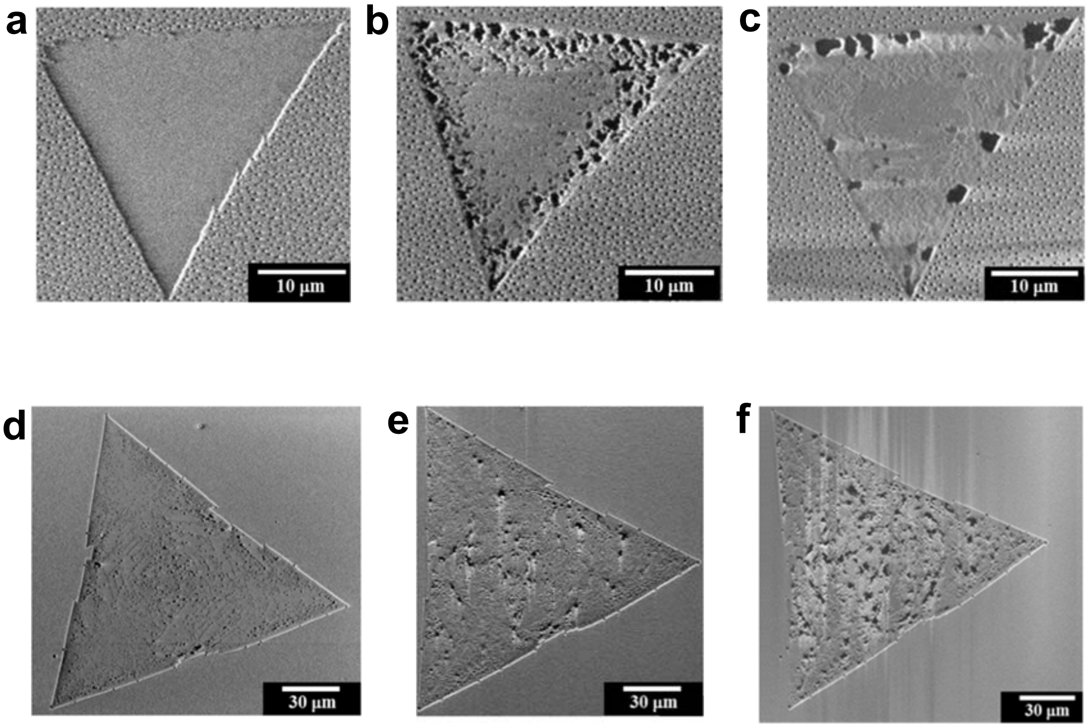

Figure S5. SEM images of a pure and a NaCl-assisted WS_2 monolayer stored under fluorescent light and 55% RH for (a,d) 1 day, (b,e) 3 days, and (c,f) 7 days, respectively.

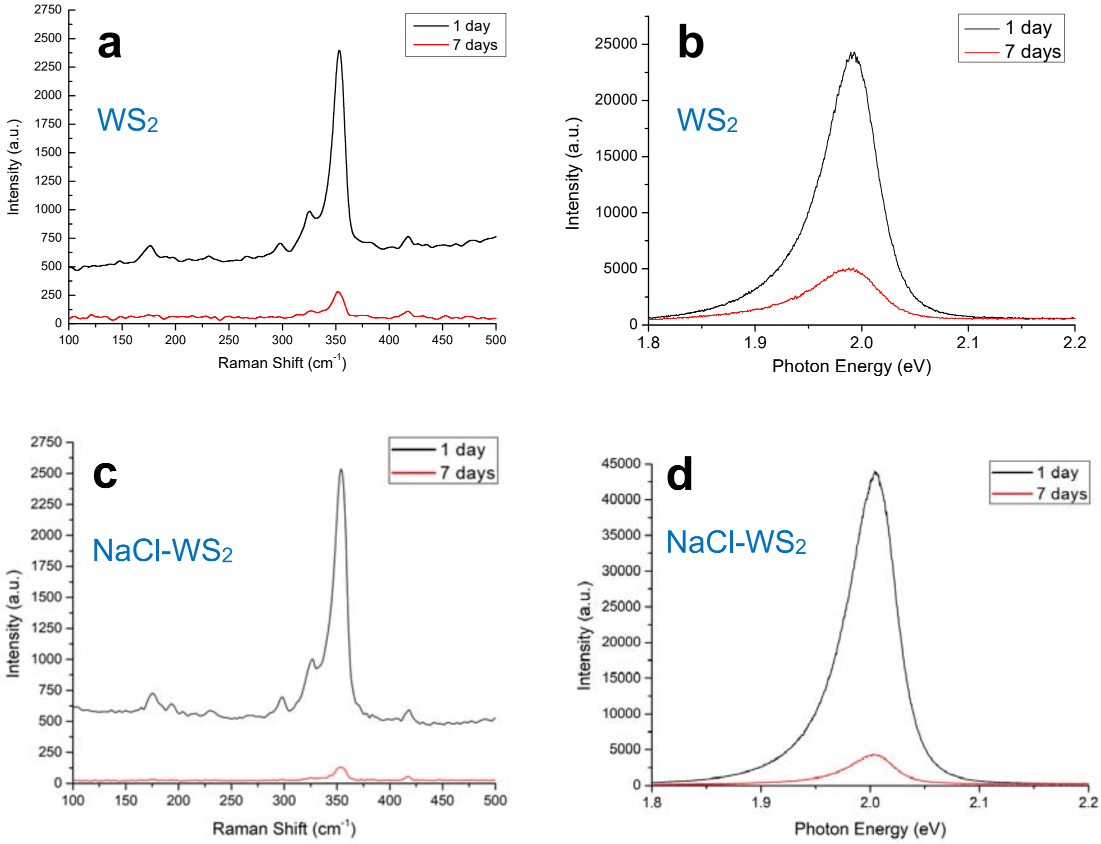

Figure S6. (a,c) Raman and (b,d) PL spectra of the WS_2 samples without and with NaCl assistant, respectively, stored under fluorescent light and 55% RH for 1 day and 7 days. The measurement point covers the black area in the SEM image (i.e., the transparent area in the optical microscopy (OM) images).

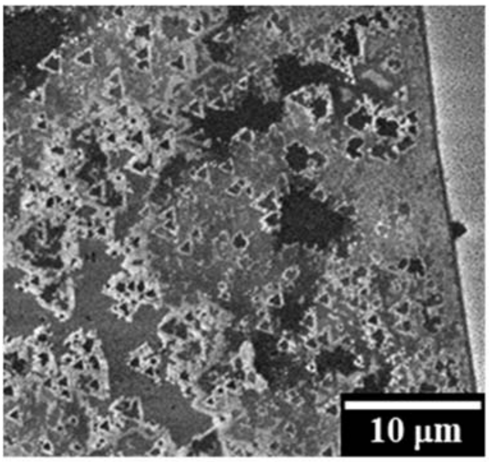

Figure S7. Magnified SEM image of the selected area of WS_2 sample with NaCl assistant stored under fluorescent light and 55% RH for 7 days. There are small triangles, which is similar to pure WS_2 caused by surface defects.[1,2,3]

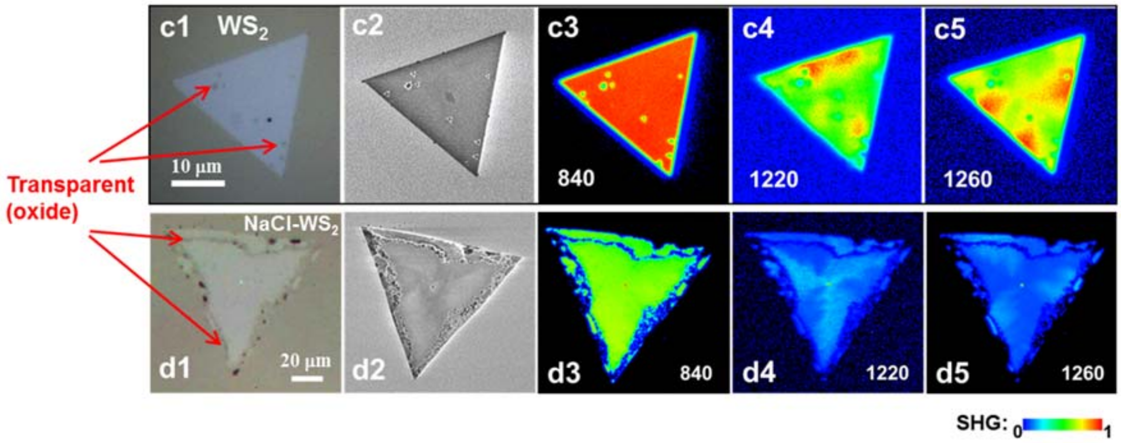

Figure S8. WS_2 and NaCl-assisted WS_2 monolayers stored under fluorescent light and 55% RH about 1 day were characterized by optical microscopy (c1,d1), SEM (c2,d2), and SHG (c3-c5,d3-d5), respectively. SHG images were excited at 840, 1220, and 1260 nm with fluence of $\sim 3.1 \times 10^6$, 4.6×10^7, and 5.1×10^7 Jm^{-2}, respectively. SHG intensity is normalized and shown with a rainbow color scale.

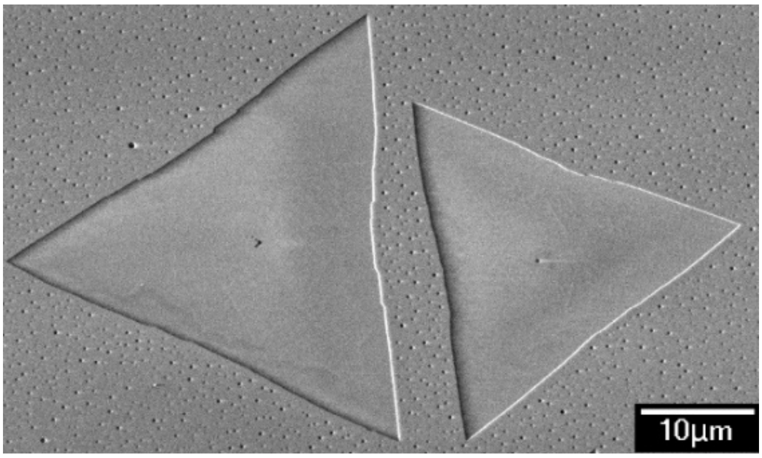

Figure S9. SEM image of the NaCl-assisted WS_2 flakes stored in a Schlenk tube pumped to vacuum (ca. 1.7×10^{-3} Torr) and exposed to fluorescent light for 14 days. There is no visible change in the NaCl-assisted WS_2 monolayers.

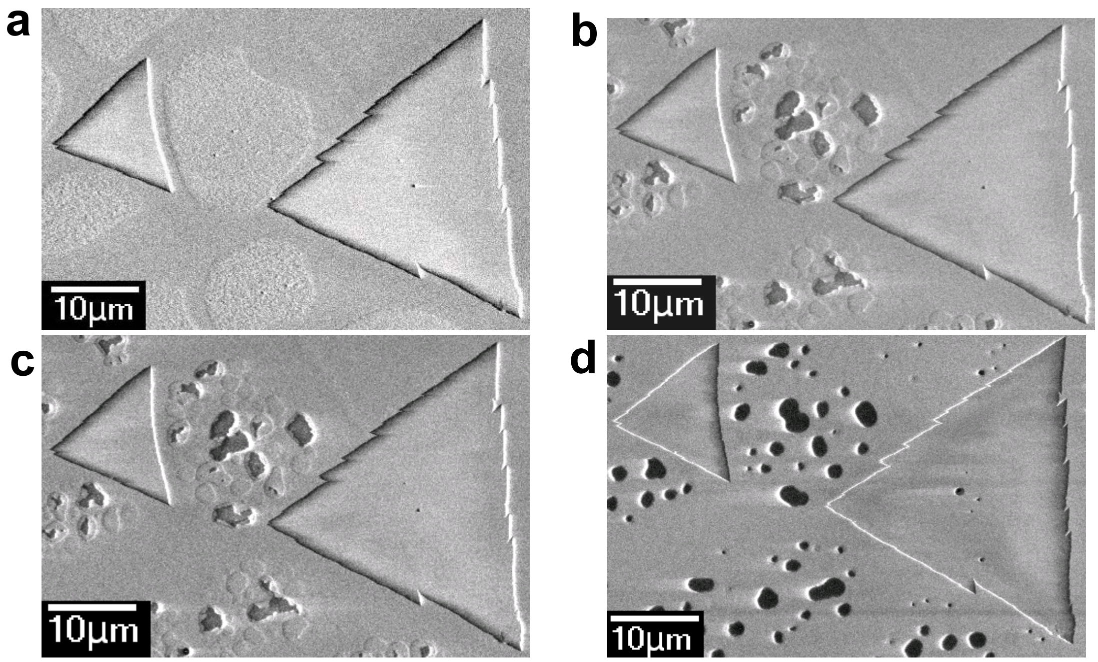

Figure S10. SEM images of pure WS_2 sample stored at dark and 99% RH for (a) 1 day, (b) 3 days, (c) 7 days, and (d) 14 days.

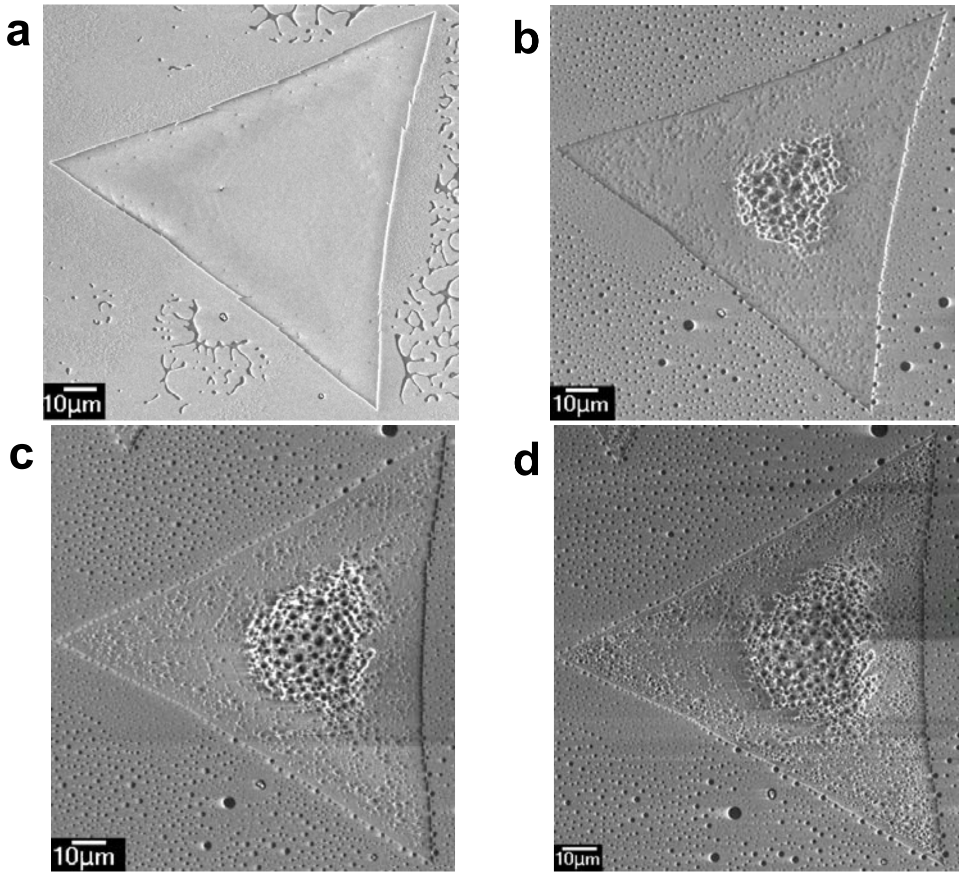

Figure S11. SEM images of WS_2 sample with NaCl assistant stored at dark and 99% RH for (a) 1 day, (b) 3 days, (c) 7 days, and (d) 14 days.

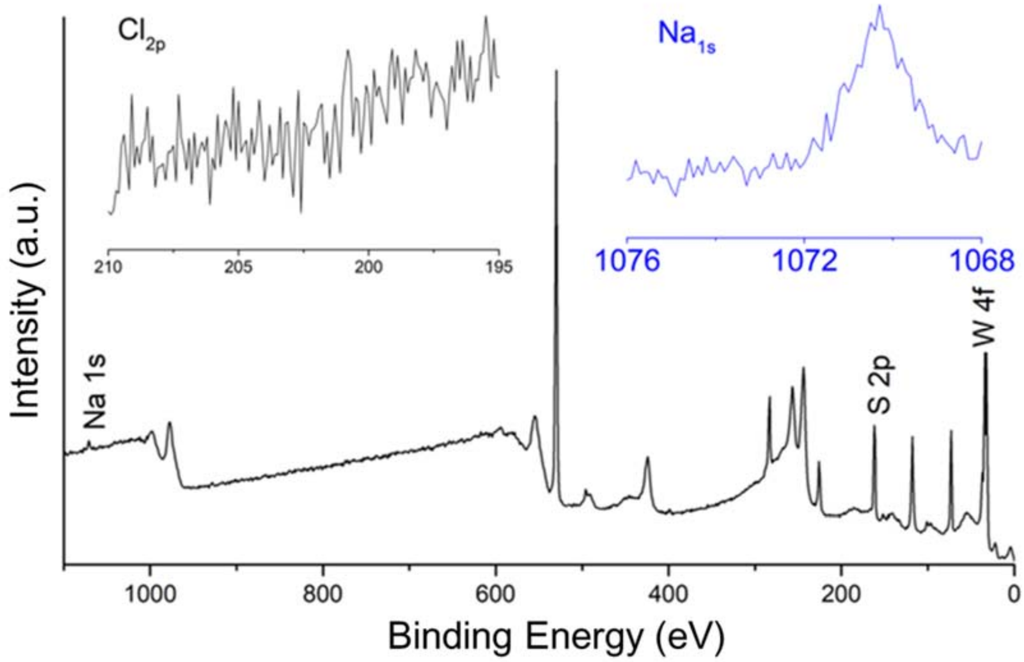

Figure S12. XPS survey spectra of the WS_2 samples grown by NaCl-assisted CVD collected after the degradation process. The insets show the high resolution XPS spectra of the energy ranges of Na1s and Cl2p. No Cl2p signal is observed.[4]

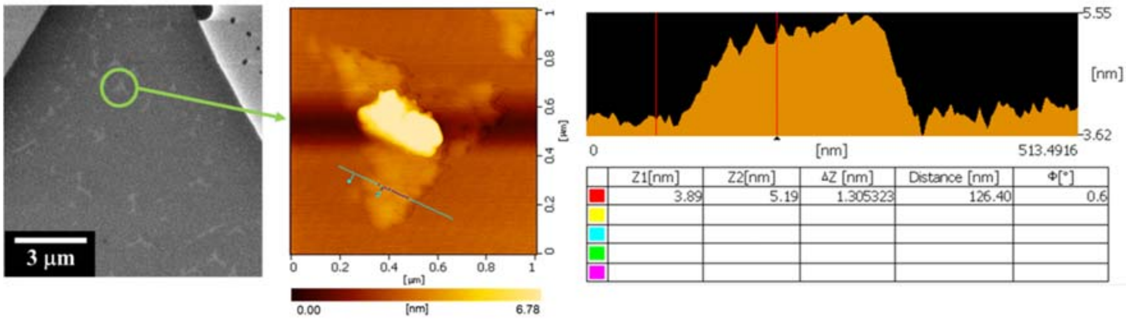

Figure S13. SEM image and enlarged AFM image of a NaCl-assisted WS_2 monolayer stored under fluorescent light and 55% RH for 1 day. There was a small raised area in the middle of the triangular oxide island. The height of this island is ~1.3 nm.

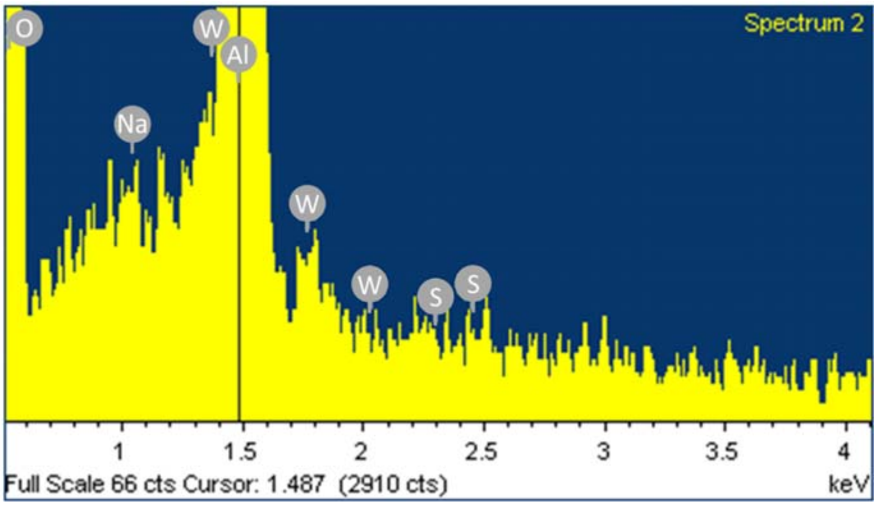

Figure S14. Energy-dispersive X-ray spectroscopy (EDS) analysis on the big dot in Figure 4g and found the presence of O, Na, W, Al, and S elements.[5,6]

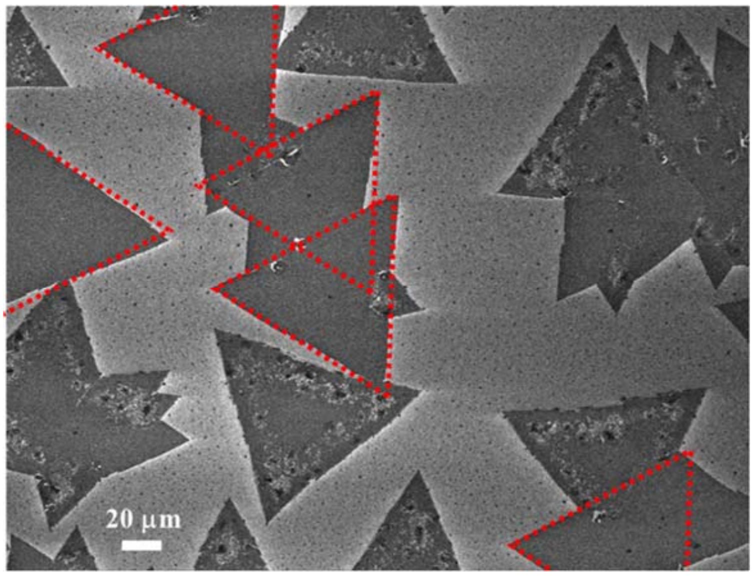

Figure S15. SEM image of the NaCl-assisted WS_2 monolayers in a specific orientation marked by red dashed triangles, which have anti-photooxidation properties.

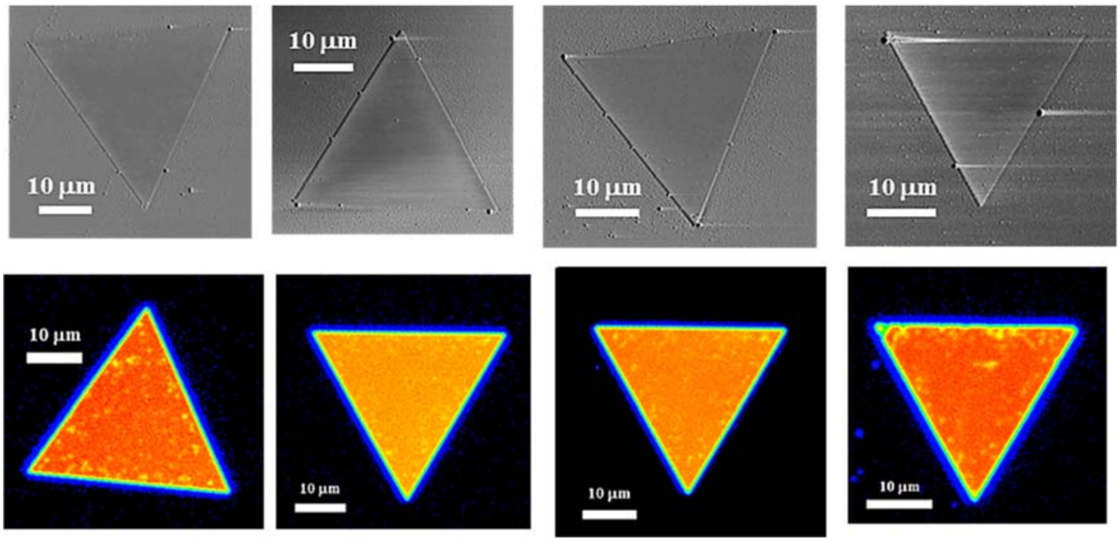

Figure S16. SEM and SHG images of Type I NaCl-assisted WS_2 flakes after 7.5 hours of fluorescent light exposure with fluence of ~4.5×10^4 Jm^{-2} at 55% RH. These are eight different flakes. These images show the photooxidation effect of WS_2 grown with 0.5 mg NaCl assistant.

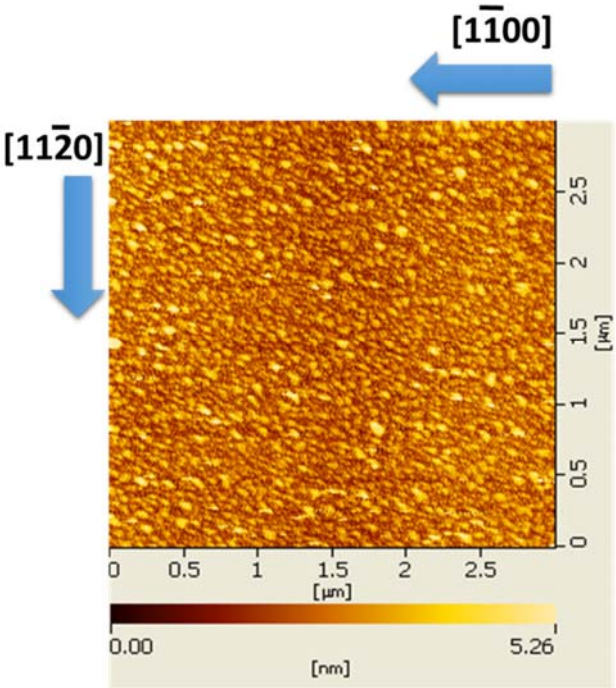

Figure S17. AFM image of the sapphire substrate, which went through a complete CVD growth process, except that WO_3 and sulfur powder precursors were not added. The growth temperature of our system is 850 ºC, which is lower than the 950 ºC indicated in the literature.[7,8] This makes the sapphire substrate not produce obvious steps.

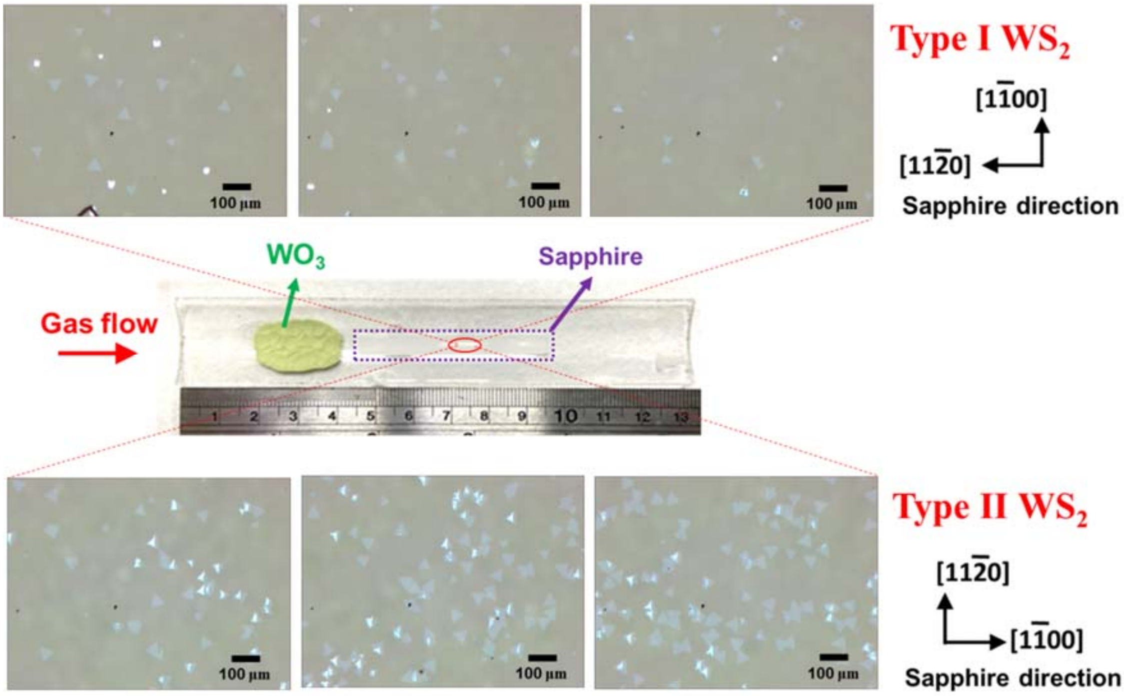

Figure S18. The OM images show the growth density of Type I and Type II WS_2. The Type II WS_2 has a higher growth density.

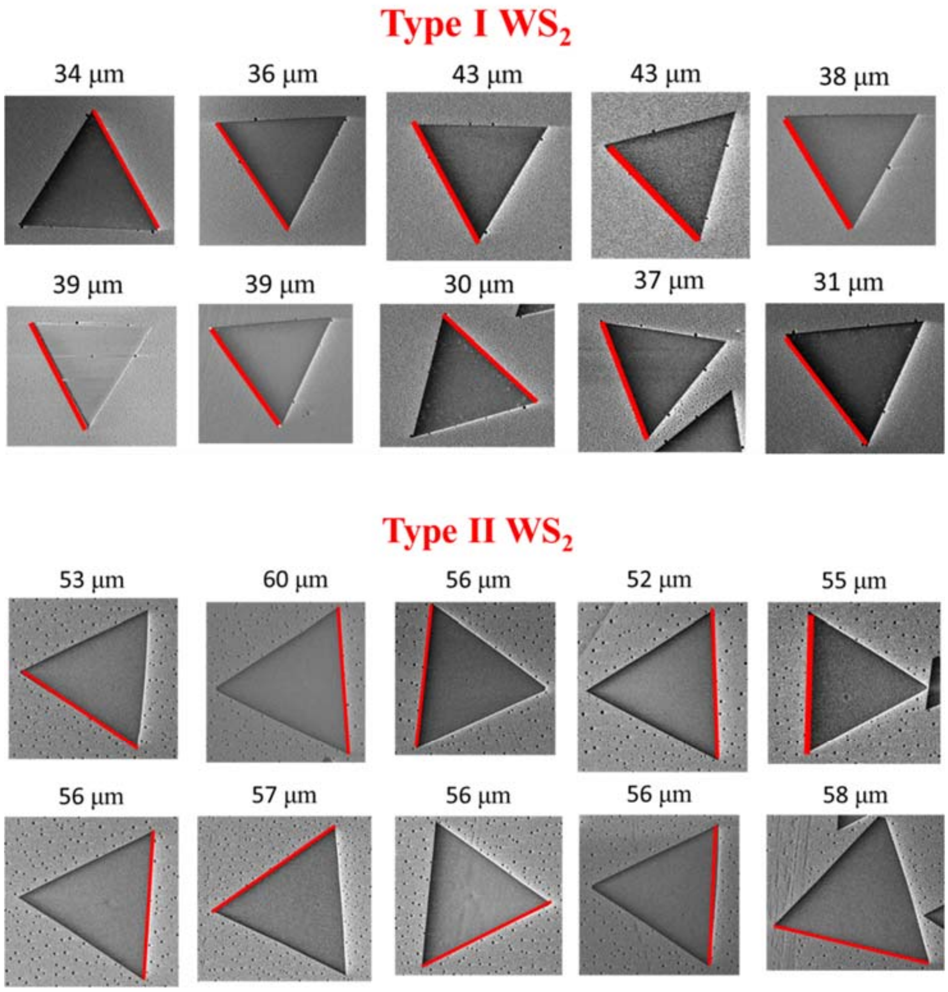

Figure S19. The sizes of Type I and Type II WS_2 are counted from the SEM images. The average size of Type I and Type II WS_2 is 37 and 56 μm, respectively. The red lines represent the side length.

References

1. Lin, Y.-C.; Li, S.; Komsa, H.-P.; Chang, L.-J.; Krasheninnikov, A. V.; Eda, G.; Suenaga, K. Revealing the Atomic Defects of WS_2 Governing Its Distinct Optical Emissions. Adv. Funct. Mater. **2018**, 28, 1704210.
2. Lin, Y. C.; Bjorkman, T.; Komsa, H. P.; Teng, P. Y.; Yeh, C. H.; Huang, F. S.; Lin, K. H.; Jadczak, J.; Huang, Y. S.; Chiu, P. W., et al. Three-fold rotational defects in two-dimensional transition metal dichalcogenides. Nat. Commun. **2015**, 6, 6736.
3. Jimmy C. Kotsakidis, Quianhui Zhang, Amadeo L. Vazquez de Parga, Marc Currie, Kristian Helmerson, D. Kurt Gaskill, Michael S. Fuhrer, Oxidation of Monolayer WS_2 in Ambient Is a Photoinduced Process, Nano Lett. **2019**, 19, 5205−5215.
4. Cai, Z.; Shen, T.; Zhu, Q.; Feng, S.; Yu, Q.; Liu, J.; Tang, L.; Zhao, Y.; Wang, J.; Liu, B.; Cheng, H.-M. Dual-Additive Assisted Chemical Vapor Deposition for the Growth of Mn-Doped 2D MoS_2 with Tunable Electronic Properties. Small **2020**, 16, 1903181.
5. Lim, Y. V.; Wang, Y.; Kong, D.; Guo, L.; Wong, J. I.; Ang, L. K.; Yang, H. Y. Cubic-shaped WS_2 nanopetals on a Prussian blue derived nitrogen-doped carbon nanoporous framework for high performance sodium-ion batteries. *J. Mater. Chem. A* **2017,** *5*, 10406–10415.
6. Rostami, S.; Azizi, S. N.; Ghasemi, S. Preparation of an efficient electrocatalyst for oxalic acid oxidation based on Ag-doped ZSM-5 nanozeolites synthesized from bagasse. *J. Electroanal. Chem.* **2017**, *788*, 235–245.
7. Liang Chen, Bilu Liu, Mingyuan Ge, Yuqiang Ma, Ahmad N. Abbas, Chongwu Zhou, Step-Edge-Guided Nucleation and Growth of Aligned WSe_2 on Sapphire via a Layer-over-Layer Growth Mode. ACS Nano **2015**, 9, 8368–8375.
8. Stefano Curiotto, Dominique Chatain, Surface morphology and composition of c-, a- and m-sapphire surfaces in O_2 and H_2 environments. Surface Science **2009**, 603, 2688–2697.